

# Controlling Oxidation Reaction on Platinum by Spin Manipulation

M.C. Escaño, T.Q. Nguyen, H. Nakanishi and H. Kasai

Department of Applied Physics, Osaka University  
2-1 Yamada-oka, Suita, Osaka 565-0871, Japan,  
clare@dyn.ap.eng.osaka-u.ac.jp  
kasai@dyn.ap.eng.osaka-u.ac.jp

## ABSTRACT

As an oxidation catalyst, platinum (Pt) is widely used in chemical and automotive industries. Thus far, the dissociative adsorption of oxygen on paramagnetic Pt crystalline surfaces is activated. Reduced activation barrier implies strongly bound dissociated oxygen atoms on surface, which is often undesirable. Our present work introduces novel means to achieve facile oxygen dissociation and at the same time weakly bound dissociated oxygen atoms on Pt surface, by changing the magnetic state of Pt (paramagnetic to ferromagnetic) via Pt/M (M: Fe,Co). Atomistic modeling of O<sub>2</sub> reaction on ferromagnetic Pt based on spin density functional theory (SDFT) and Monte-Carlo simulation reveal emergence of non-activated dissociation on Pt/Fe, lower activation barrier on Pt/Co, lower binding energy of separated O atoms on Pt/M and a Pt layer magnetic phase transition beyond room temperature. The same trend in effective O-O bond elongation for molecular adsorption is observed on Pt/Co.

**Keywords:** oxygen, platinum, surface magnetism, surface reaction

## 1 INTRODUCTION

The oxidation of metal surfaces is a phenomenon that plays a central role in chemical, electrochemical and automotive industries. Key initial elementary steps in the oxygen-metal interaction is the molecular and/or dissociative adsorption. As an oxidation catalyst, Pt is widely studied in surface science. Thus far, the dissociative adsorption of O<sub>2</sub> on low-index Pt surfaces is activated and that the dissociated oxygen atoms (O<sub>ad</sub>) are strongly bound on the surface [1-3]. Reduction of the binding energy of O<sub>ad</sub> proved to be useful, from technological point of view, especially in the case where the O<sub>ad</sub> is an intermediate specie. A weakly bound O<sub>ad</sub> has been attained in various Pt monolayer bimetallic structures (MBS) [4,5] employing 3d transition metals as substrates. In the same way, the stability of oxygen molecule is decreased in Pt MBS. Generally, this is due to the broadening and lowering of the Pt d-band as a result of a shorter interlayer separation between Pt and the 3d substrates as compared to the pure Pt slab [5,7]. While the energetics of oxygen reaction on

different facets of Pt and on electronically modified Pt MBS have been extensively investigated, the influence of the magnetic state of the metal surface on the geometric, energetics, electronic and magnetic structure of the adsorbate has not been explored. There have been reports on the facile oxygen dissociation on Pt “skin” on Co and Fe substrates based on half-cell experiments [8,9]. But because to some extent, such electrochemical systems render complex reaction processes, the intrinsic role of the substrates in altering Pt surface reactivity has not been systematically studied. Moreover, studies on magnetic phases of oxygen molecular assemblies or oxide structures on non-magnetic surfaces reveal interesting ferromagnetic or antiferromagnetic interactions depending on the coverage [10-12], but so far, the change in magnetic interactions due to the modification of the surface itself has not been investigated. In this work, we present the new adsorption properties of O<sub>2</sub> on ferromagnetic Pt. We discuss the O<sub>2</sub>-Pt interaction which can form basis of further experimental and theoretical investigations on either the catalytic properties of “magnetically” modified metal surfaces for both chemical and electrochemical reactions, or for various magnetic phenomena of oxygen structures on metal surfaces.

## 2 COMPUTATIONAL METHODS

The first principles calculations performed in this study are based on spin-polarized total energy calculations within density functional theory [13,14] framework using Projector Augmented Wave (PAW) method [15] and plane-wave basis set, as implemented in Vienna *ab initio* Simulation Package (VASP) [16-19]. The ferromagnetic Pt is modeled by a Pt overlayer on magnetic substrate, M (where M: Fe,Co). The generalized gradient approximation (GGA) based on the Perdew, Burke and Ernzerhof (PBE) functional [20,21] is used for the exchange-correlation correction. Brillouin-zone integrations are performed on a grid of (4x4x1) Monkhorst-Pack k points with a Methfessel-Paxton smearing method [22]. The M substrates are modeled by a five-layer bcc(001) slab in a (2x3) super cell. The Pt atoms are pseudomorphically laid on the M substrate, forming the Pt monolayer. Each slab is separated by ~12.0Å of vacuum. The paramagnetic Pt is modeled by a four-layer fcc Pt(100)-(1x1) slab, which exhibits the same

surface structure as that of the ferromagnetic Pt layer. The optimized Pt/M surface is obtained by relaxing the Pt layer and the two top-most layers of the substrates using the conjugate gradient method. The plane-wave expansion with a cutoff of 400 eV is used throughout the calculations. The temperature dependence of the magnetization of the Pt layer is determined using a combination of DFT calculations and Monte Carlo simulations. The interlayer exchange parameters are obtained by constrained density functional theory [23]. In this method, a set of non-collinear magnetic configurations are derived by fixing the local moment direction of Pt and M atoms in non-equilibrium directions via a constraining field and the energy dependence on the orientation of spins can be mapped onto Heisenberg model to extract the interlayer exchange parameters, which are then used in the Monte Carlo (MC) simulation to study the finite-temperature magnetic properties. For the MC simulation, the standard Metropolis algorithm is carried out within  $\sim 200,000$  MC steps and a system size of  $(L \times L \times n) = 20 \times 20 \times 6$ , where  $n$  is the number of atomic planes and where  $L \times L$  gives the atomic sites in a plane. A two-dimensional periodic boundary conditions with free boundary condition (perpendicular to the plane) are adopted.

### 3 RESULTS AND DISCUSSIONS

#### 3.1 Ferromagnetic Pt

We show in Figure 1 the schematic diagram representing the induced spin moment on Pt site due to substrate, M. The optimized Pt layer distance from the M substrate is 1.62-1.63Å. This is 0.30Å shorter than that of paramagnetic Pt, which is consistent with stronger Pt-M binding in the order of  $\sim 0.29$ eV. The Pt-M binding energy is defined as one Pt atom vacancy formation energy. We can therefore expect a lower d-band for the Pt layer as compared to the pure Pt due this stronger Pt-M binding. Since the lattice mismatch between the Pt layer and the substrates is very small ( $\sim 0.4$ - $0.5\%$ ), then the Pt layer is considered unstrained, which is consistent with experimental observations on layer-by-layer epitaxial growth of Pt on M [24,25]. An induced magnetic moment of  $0.62\mu_B$  and  $0.43\mu_B$  on Pt layer on Fe and Co substrates, respectively, is obtained based on the sphere cut-off of 1.455Å for the integration of magnetization density. The induced magnetization of Pt has been experimentally observed in Pt/Fe and in Pt/Co layered structures (LS) [24,25]. The calculated room temperature magnetic moment of Pt is  $0.53\mu_B$ , in excellent agreement with the X-ray magnetic circular dichroism (XMCD) result for Pt/Fe bimetallic system ( $0.50\mu_B$ ) [25], while the calculated magnetic moment of Pt in Pt/Co at room temperature is  $0.22\mu_B$ , which is in agreement with XMCD of Pt in Pt/Co(001) LS ( $0.20\mu_B$ ) [24]. The temperature dependence of the magnetization of Pt layer, 6 monolayers of bcc Fe(001) and Pt/Fe is shown in Figure 2. Based on the temperature dependence on magnetic susceptibility, we

found that the magnetic phase transition temperature for Pt on Fe is 403K and for Pt on Co is 354K. The origin of magnetic property of an unfilled 5d-shell, which is nonmagnetic in pure metal, is usually understood in terms of strong mixing of 5d-states with M 3d-states, giving a spin-splitting of electronic states near the Fermi level ( $E_F$ ). We also observed the same phenomenon for pure Pt. We note that the spin-splitting changes the character of the d-orbitals. For instance, the spin-down  $d_{zz}$  state, which is filled in pure Pt is shifted towards the  $E_F$  in Pt/M (Figure 3) [26-28].

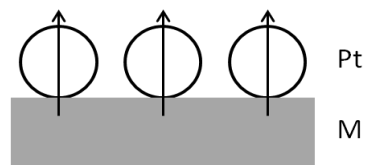


Figure 1: Spin moment induced at Pt site due to substrate, M (where M:Fe,Co).

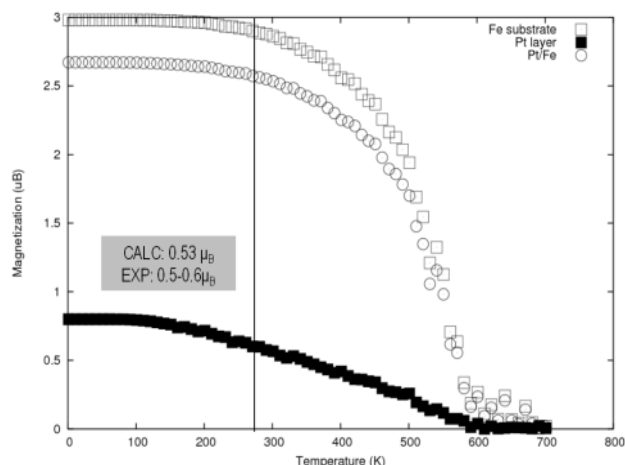


Figure 2: Temperature dependence of magnetization of Pt/M.

#### 3.2 O<sub>2</sub> dissociative adsorption

To compare the O<sub>2</sub> dissociative adsorption among the three systems, we considered two important regions in potential energy plot shown in Figure 4. The potential energy curves represent the oxygen dissociative adsorption energetics. This dissociation favors the bridge-hollow-bridge (*b-h-b*) pathway as shown in the inset figure. A non-activated dissociative adsorption is noted in Pt/Fe. The potential minimum is designated as 2O<sub>ad</sub> binding energies. The trend in these binding energies is: Pt ( $-2.40$ eV) > Pt/Co ( $-1.40$ eV) > Pt/Fe ( $-1.33$ eV). However, the binding energy at the transition state (TS) is in the following order: Pt ( $0.16$ eV) >

Pt/Co (0.11) > Pt/Fe (0.00eV). A lower activation barrier for oxygen dissociation on Pt/M also gives lower stability of dissociated species. We think that the spin-polarization of Pt due to M resulting to spin-polarized d-state near or at  $E_F$  (discussed previously), promotes effective hybridization with antibonding states of oxygen, enhancing O-O bond elongation.

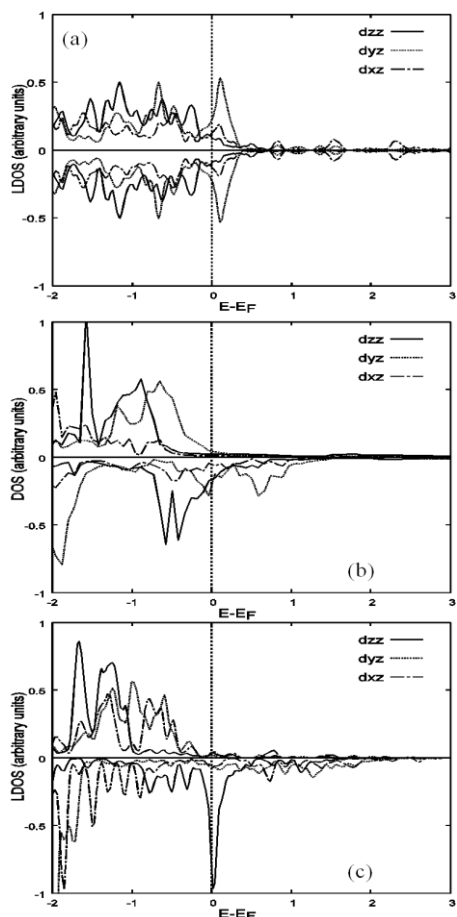


Figure 3: Spin-polarization of Pt d-states in (b) Co and (c) Fe as compared to (a) pure Pt.

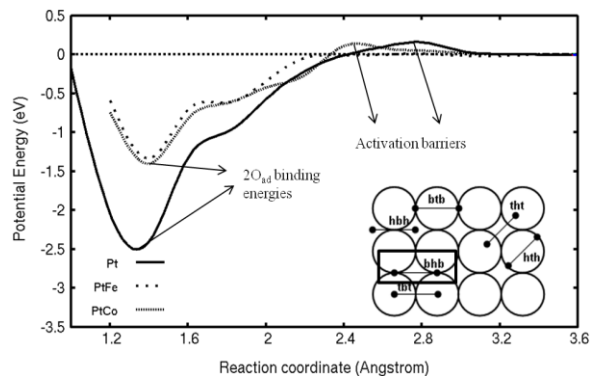


Figure 4: Potential energy curves for oxygen dissociative adsorption on Pt, Pt/Co and Pt/Fe.

## 4.1 Molecular adsorption

We found the same most stable molecular configuration of oxygen (top-bridge-top or *t-b-t*) on both ferromagnetic Pt and paramagnetic Pt. The *t-b-t* configuration is shown in Figure 5. The oxygen center of mass is over the bridge site and the O-O internuclear axis spans toward the Pt top sites. The O-O bond elongation on Pt/Co is 0.01 Å greater than that of paramagnetic Pt, despite the much lower adsorption energy in the former. The effective O-O bond elongation is mainly due to spin-polarization of Pt layer on M. The spin-splitting of d-states renders a closer spin-down  $d_{zz}$  states to  $E_F$  than in paramagnetic counterpart. The magnetic moment of  $O_2$  on Pt/Co is lower than that of Pt by  $\sim 0.02\mu_B$ . The O-O stretching frequency is  $890\text{cm}^{-1}$ , while that of paramagnetic Pt is  $893\text{cm}^{-1}$ , suggesting that the molecularly adsorbed state is superoxo  $-$ type. This is in agreement with the  $O_2$  molecular state assignments using vibrational spectroscopies [29-31].

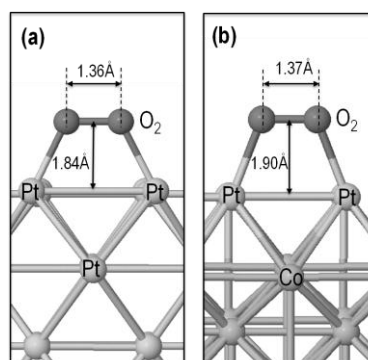


Figure 4: Molecular oxygen adsorption on (a) Pt and (b) Pt/Co showing the geometry and the *t-b-t* adsorption configuration.

## 4 CONCLUSION

We carried out first principles calculations based on DFT-GGA to determine the changes in dissociative adsorption energy profile of  $O_2$  and the modification in the geometry, energetics, electronic and magnetic properties of molecularly adsorbed oxygen as a result of the change in the magnetic state of Pt surface. We found that the most favorable pathway for  $O_2$  dissociative adsorption is *b-h-b* site and the same most stable molecular configuration is *t-b-t* on both ferromagnetic Pt (modeled by Pt/M) and paramagnetic Pt {represented by Pt(100)-(1x1)}. The effective O-O bond elongation on Pt/M, despite the much lower adsorption energy, is due to spin-polarization of Pt layer on M. The spin-splitting of d-states renders a closer spin-down  $d_{zz}$  states to  $E_F$  than in paramagnetic counterpart. The temperature dependence of the

magnetization of Pt layer obtained by a combination of DFT and MC simulations reveal that such properties can be retained until the magnetic phase transition temperature of 354K for Pt on Co and 403K for Pt on Fe.

### Acknowledgment

This work is supported by the Special Coordination Funds for the Global Center of Excellence (COE) program (H08) "Center of Excellence for Atomically Controlled Fabrication Technology. Some of the calculations were done using computer facilities of the Cyber Media Center (Osaka University), the ISSP Super Computer Center (University of Tokyo). M.C. Escaño would like to extend gratitude to Japan Society for Promotion of Science (JSPS) Fellowship and T.Q. Nguyen would like to thank Ministry of Education, Culture, Sports, Science and Technology of Japan (MEXT) for research funds.

### REFERENCES

- [1] A.C. Luntz, M.D. Williams, D.S. Bethune, J. Chem. Phys. 89, 4381(1988).
- [2] A.C. Luntz, J. Grimblot, D.E. Fowler, Phys. Rev. B 39, 12903 (1989).
- [3] W. Wurth, J. Stöhr, P. Feulner, X. Pan, K.R. Bauchspiess, Y. Baba, E. Hudel, G. Rucker, D. Menzel, Phys. Rev. Lett. 65, 2426 (1990).
- [4] C. Puglia, A. Nilsson, B. Hernnäs, O. Karis, P. Bennich, N. Martensson, Surf. Sci. 342,119 (1995).
- [5] V.A. Sobyenin, G.K. Boreskov, A.R. Cholach, A.P. Losev, React. Kinet. Catal. Lett. 27, 299 (1985).
- [6] J. R. Kitchin, J. K. Nørskov, M. A. Barteau, J. G. Chen J. Chem Phys. 120, 21(2004).
- [7] J.G. Chen, C.A. Menning, M.B. Zellner, Surf. Sci. Rep. 63, 201 (2008).
- [8] J. Zeng, S. Liao, J. Y. Lee, Z. Liang Int. J. of Hydrogen Energ. 35, 942 (2010).
- [9] M. Wakisaka, H. Suzuki, S. Mitsui, H. Uchida and M. Watanabe J. Phys. Chem. C 112, 2750 (2008).
- [10] Y. Kunisada, M.C. Escaño, H. Kasai. J. Phys.: Condens. Matt. 23, 394207 (2011).
- [11] H. Suematsu, Y. Murakami J. of Magn. Magn. Mater. 90 & 91, 749 (1990).
- [12] M. Otani, H. Miyagi, N. Suzuki Physica B 265, 60 (1999).
- [13] P. Hohenberg, W. Kohn, Phys. Rev. 136, B864 (1964).
- [14] W. Kohn, L.J. Sham, Phys. Rev. 140, A1133(1965).
- [15] G. Kresse, J. Joubert, Phys Rev. B 59, 1758 (1999).
- [16] G. Kresse, J. Furthmüller, Comput. Mater. Sci. 6,15 (1996).
- [17] G. Kresse, J. Furthmüller, Phys. Rev. B 54, 11169 (1996).
- [18] G. Kresse, J. Hafner, Phys. Rev. B 47, 558 (1993).
- [19] G. Kresse, J. Hafner, Phys. Rev. B 49, 14251 (1994).
- [20] J. P. Perdew, K. Burke, M. Ernzerhof, Phys. Rev. Lett. 77, 3865 (1996).
- [21] J. P. Perdew, K. Burke, M. Ernzerhof, Phys. Rev. Lett. 78, 1396 (1997).
- [22] M. Methfessel, A. Paxton, Phys. Rev. B 40, 3616 (1989).
- [23] P.H. Dederichs, S. Blügel, R. Zeller, H. Akai, Phys. Rev. Lett. 53, 2512 (1984).
- [24] A. Wachter, K.P. Bohnen, K.M. Ho Ann. Physik 6, 215 (1996).
- [25] S.M. Valvidares, T. Schroeder, O. Robach, C. Quiros, T.L. Lee and S. Ferrer Phys. Rev. B 70, 224413 (2004).
- [26] M.C. Escaño, T.Q. Nguyen, H. Nakanishi and H. Kasai, Surf. Sci. 602, 3415 (2008).
- [27] M.C. Escano, T.Q. Nguyen, H. Nakanishi, H. Kasai. J. Phys.: Condens. Matt. 21, 49221 (2009).
- [28] M.C. Escaño, H. Nakanishi and H. Kasai, J. Phys. Chem. A 113, 14302 (2009).
- [29] C.T. Campbell, G. Ertl, H. Kuiper, and J. Segner, Surf. Sci. 107, 220 (1981).
- [30] N.R. Avery Chem. Phys. Lett. 96, 371 (1983).
- [31] V.A. Sobyenin, K.I. Zamaraev React. Kinet. Catal. Lett. 31, 273 (1986).